


MODELING OF PARALLEL MANIPULATORS WITH FLEXIBLE LINKS AND JOINTS DRIVEN BY ELECTRIC ACTUATORS

Nguyen Quang Hoang¹, Benjamin Boudon², Hyun-Jun BAE²,
Thu Thuy DANG², Chedli Bouzgarrou²

¹*Department of Mechatronics/Applied Mechanics, School of Mechanical Engineering, Hanoi University of Science and Technology, Hanoi, Vietnam*

²*Université Clermont Auvergne, CNRS, SIGMA Clermont, Institut Pascal, F-63000 Clermont-Ferrand, France*

*E-mail: hoang.nguyenquang@hust.edu.vn

Received: 09 December 2022 / Published online: 30 December 2022

Abstract. This paper presents the approach of building a mathematical model for a parallel robotic manipulator with flexible links and elastic joints. The links to the base are assumed to be rigid bodies, and the thin connecting rods are assumed to be flexible links. The elasticity of the transmission from the actuators to the transmission is modeled by a torsional spring and viscous damper. This is a mixed system of rigid bodies, spring, and flexible links. The deformation motion of the elastic link is approximated by shape functions similar to the finite element method. The differential equations of motion are established by combining the substructure method and the Lagrange equation of the 2nd kind for the serial multibody system. Based on the differential equation established for the parallel robot manipulator of five bars, numerical simulations were carried out to investigate the response of the system.

Keywords: parallel robot manipulator, elastic links, elastic joints, modeling, numerical simulation.

1. INTRODUCTION

In the era of the fourth industrial revolution, mechatronics and robotics are playing an increasingly important role. Compared with the serial robot manipulator, the parallel robot manipulator has the following advantages: higher accuracy, because the error between the pins is compensated for each other without having to accumulate; the mass of the moving link is lighter; better stability. Although the disadvantages of parallel robots are that the workspace is smaller and they require more complex analysis of singularities than serial robots, they are often preferred for high speed and high-precision tasks. The efficiency of the robot is not only to be more accurate and faster, but also to be lighter

and consume less energy. This fact leads that the slender link is no longer considered as a rigid body but as an elastic link, which takes into account the elastic deformation of the links. In addition, when the robot has a large acceleration, the elasticity of the transmission also needs to be considered.

The study of flexible manipulators has attracted the attention of scientists in the last three decades. There have been many studies on the dynamics and control of manipulators with flexible links. These works are summarized in review articles such as [1–6]. In general, they focus on modeling, calculation of dynamics and oscillation, and control design for flexible manipulators. The research works presented in [3, 7–11] focus on elastic serial robotic manipulators. Other works [12–16] concern closed loop multi-body systems to study parallel robots with elastic links in which, five main methods are used to model elastic links including: (1) Lumped parameter method [17], (2) Finite difference method [18], (3) Method of expansion to assumed mode functions [7, 10, 12, 13, 16, 19–25], (4) Finite element method [9, 11, 14, 26, 27], (5) Method of multibody systems [8]. Each method has its advantages and disadvantages, which method to use depends on forte and supporting tools.

In this paper, the finite element method and Lagrange equation of 2nd kind are used to build a dynamic model for a parallel planar manipulator with elastic links and joints. Based on the equations of motion, it is possible to simulate the response of the system to the conventional PD controller for the positioning problem. The remainder of this paper is organized as following: Section 2 describes the structure diagram of the manipulator from actuators to the end effector. Section 3 presents the establishment of a dynamic model for the system, in which the equations of motion for one part is developed in detail. Section 4 presents the numerical simulation results of the forward dynamics. The conclusion is made in the final section.

2. ELECTROMECHANICAL MODEL OF A FIVE-BAR PARALLEL ROBOT WITH FLEXIBLE LINKS AND JOINTS

Consider a 5-bar planar parallel manipulator driven by two DC motors as shown in Fig. 1. The two links connected to the base are considered as rigid bodies, the two slender rods connected to the end point E are flexible links, and the transmission of the active joints are also considered elastic ones.

The system parameters include:

- DC motor: resistance R_a , inductance L_a , torque constant K_m , back-emf constant K_e , inertia of the rotor I_m ;
- Gear transmission: r – gear ratio, its mass is neglected;
- Torsional stiffness of the shaft k , torsional damping c ; linear damping at the shaft d ;
- Links connected to the base: length of l_1 , mass m_1 , moment of inertia about the axis of rotation I_1 , center of mass at the middle point;
- Flexible links: length of l_2 , cross-sectional area $b \times h$, mass density ρ , elastic module E ;

To establish the dynamic equation for this robotic manipulator, we combine the substructure method and the Lagrange equation of the 2nd kind. Imagine that the joint E is cut and two reaction forces are added at E of each part. Two parts are then treated as serial manipulators with elastic joints and link, Fig. 2. The dynamic equations for the two parts are similar. Therefore, only the deriving equations of motion for the right part is presented in detail.

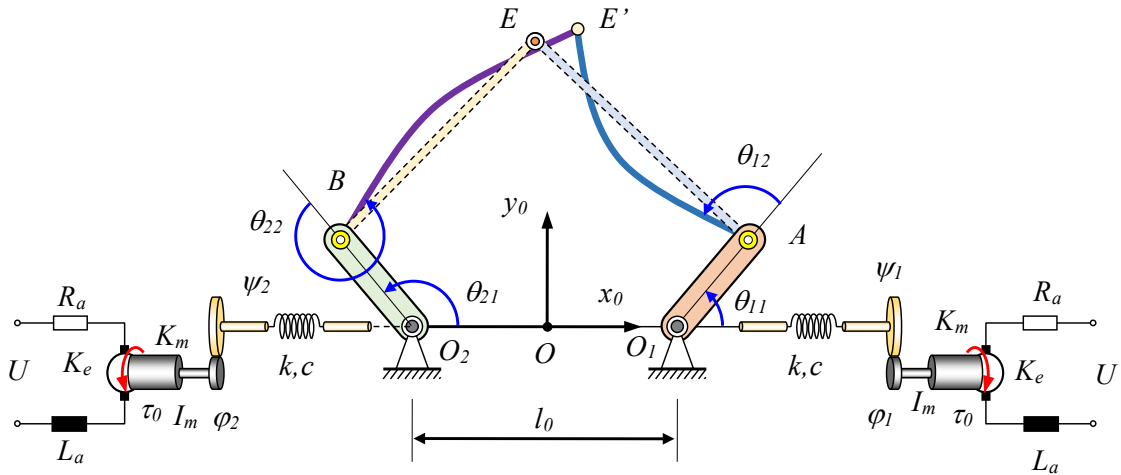


Fig. 1. Five-bar parallel robot with flexible links and joints

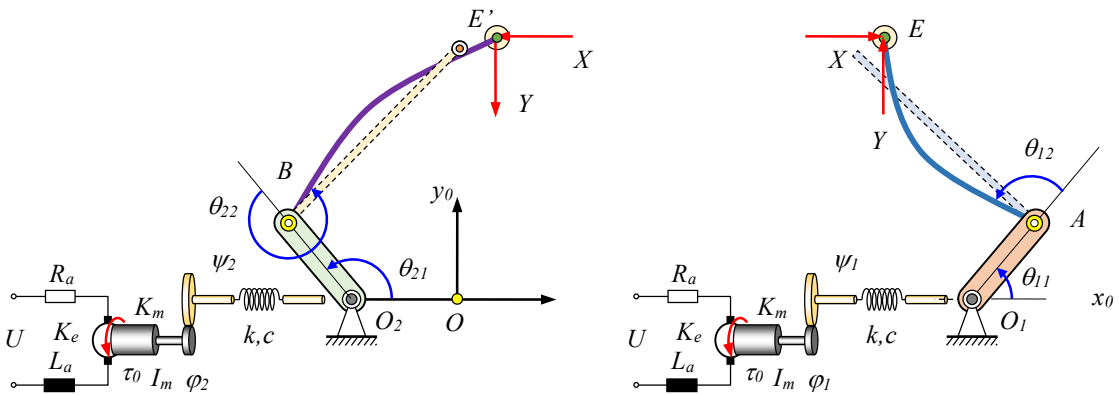


Fig. 2. Substructure diagram

Description of the deformation motion of the elastic link

To describe the deformation motion of elastic link AE, we introduce a floating coordinate system Axy (frame 1). The origin A is fixed to one end of the link and axis Ax tangential to the link at end A, Fig. 3. Denote $[\vec{i}, \vec{j}]$ are two unit vectors of the coordinate

system Axy . The displacement due to deformation of point P at a distance $x = \xi$ from A is determined by

$$\vec{d} = w(x, t)\vec{j},$$

where $w(x, t)$ is the transverse displacement due to bending deformation.

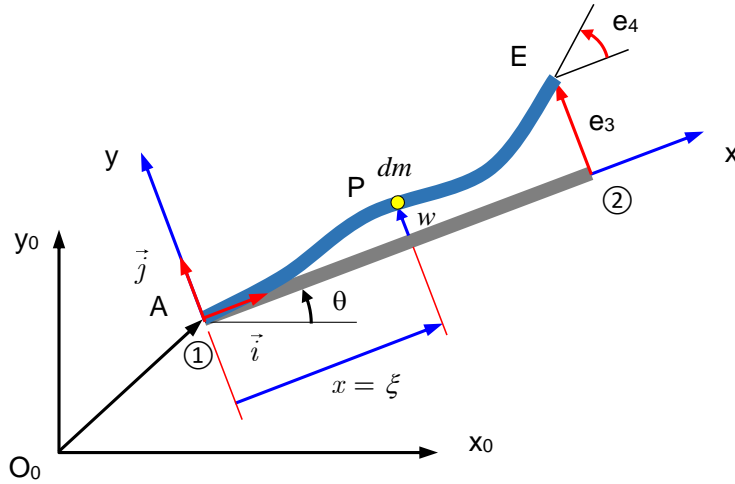


Fig. 3. Motion presentation of flexible link

Here the approach of FEM (finite element method) is applied. Each flexible link will be considered as a beam. Let $[e_3, e_4]$ be transverse and angular displacements of node 2 (end 2) respectively, the displacement of point P is determined through the following shape functions (displacements at end A are 0, $[e_1, e_2]^T = \mathbf{0}$)

$$w(x) = h_3(x)e_3 + h_4(x)e_4 = \begin{bmatrix} h_3(x) & h_4(x) \end{bmatrix} \begin{bmatrix} e_3 \\ e_4 \end{bmatrix} = \mathbf{S}(x)\mathbf{e}, \quad 0 \leq x \leq l. \quad (1)$$

The shape functions are chosen by polynomials as the following

$$h_3(x) = \frac{1}{l^3}(-2x^3 + 3lx^2), \quad h_4(x) = \frac{1}{l^2}(x^3 - lx^2). \quad (2)$$

In the floating frame Axy , the position of the point P is determined as

$$\mathbf{r}_P^{(1)} = \begin{bmatrix} x \\ \mathbf{S}(x)\mathbf{e} \end{bmatrix}. \quad (3)$$

The coordinates of the point P belonging to the elastic link in the fixed frame are determined

$$\mathbf{r}_P^{(0)} = \mathbf{r}_A^{(0)} + \mathbf{R}(\theta)\mathbf{r}_P^{(1)}, \quad (4)$$

where the rotation matrix is defined by

$$\mathbf{R}(\theta) = \begin{bmatrix} \cos \theta & -\sin \theta \\ \sin \theta & \cos \theta \end{bmatrix}.$$

The results of (4) are written in detail as

$$\begin{aligned}x_p^{(0)} &= x_A + x \cos \theta - w(x, t) \sin \theta, \\y_p^{(0)} &= y_A + x \sin \theta + w(x, t) \cos \theta.\end{aligned}\quad (5)$$

The coordinates of the endpoint E in the fixed system are determined

$$\begin{aligned}x_E^{(0)} &= x_A + l \cos \theta - e_3 \sin \theta, \\y_E^{(0)} &= y_A + l \sin \theta + e_3 \cos \theta.\end{aligned}\quad (6)$$

Now, we can choose generalized coordinates of two parts as:

$$\begin{aligned}\mathbf{q}_1 &= [\mathbf{q}_{1r}^T, \mathbf{q}_{1e}^T]^T = [\varphi_1, \theta_{11}, \theta_{12} | e_{13}, e_{14}]^T \text{ - for the right part,} \\ \mathbf{q}_2 &= [\mathbf{q}_{2r}^T, \mathbf{q}_{2e}^T]^T = [\varphi_2, \theta_{21}, \theta_{22} | e_{23}, e_{24}]^T \text{ - for the left part,}\end{aligned}$$

where $\varphi_k, \theta_{k1}, \theta_{k2}$ are angular position of rotors, of the rigid link, and relative angle of flexible link w.r.t to the rigid link (Fig. 1); e_{k3}, e_{k4} are transverse and angular deformation at the end of the flexible links, $k = 1, 2$ (Fig. 3).

3. EQUATIONS OF MOTION

In this section, the equations of one part are established using Lagrange equations of the second kind. The procedure is the same for serial manipulators. Here, we need to calculate the kinetic, potential, dissipative energy of the system, and control torques. Two parts obtained after decoupling joint E have the same structure, so in the following only equations of motion of the right part are presented.

3.1. Kinetic energy – mass matrix

The right part consists of the rotor, the rigid link OA and the flexible link AE. The kinetic energy of this part is calculated as

$$T = \frac{1}{2} I_m \dot{\varphi}_1^2 + \frac{1}{2} I_{10} \dot{\theta}_{11}^2 + T_{AE} + T_{tip}.$$

The kinetic energy of the rotor and the rigid link OA is given by

$$T_r = \frac{1}{2} I_m \dot{\varphi}_1^2 + \frac{1}{2} I_{10} \dot{\theta}_{11}^2 = \frac{1}{2} \dot{\mathbf{q}}_1^T \mathbf{M}_r \dot{\mathbf{q}}_1,$$

with $\mathbf{M}_r = \text{diag}([I_m, I_{10}, 0, 0, 0])$.

The kinetic energy of the flexible link AE is calculated by

$$T_{AE} = \frac{1}{2} \int v^2 dm = \frac{1}{2} \frac{m_2}{l_2} \int_0^{l_2} v^2 d\xi,$$

where v is velocity of the infinitesimal mass dm belonging to link AE. The coordinates of the point P belonging to the elastic link in the fixed frame are determined

$$\begin{aligned} x_P^{(0)} &= x_A + x \cos \theta - w(x, t) \sin \theta \\ &= x_{O_1} + l_1 \cos \theta_{11} + x \cos(\theta_{11} + \theta_{12}) - w(x, t) \sin(\theta_{11} + \theta_{12}), \\ y_P^{(0)} &= y_A + x \sin \theta + w(x, t) \cos \theta \\ &= y_{O_1} + l_1 \sin \theta_{11} + x \sin(\theta_{11} + \theta_{12}) + w(x, t) \cos(\theta_{11} + \theta_{12}). \end{aligned}$$

Using (1), we get

$$\begin{aligned} x_P^{(0)} &= x_{O_1} + l_1 \cos \theta_{11} + x \cos(\theta_{11} + \theta_{12}) - \mathbf{S}(x) \mathbf{e} \sin(\theta_{11} + \theta_{12}), \\ y_P^{(0)} &= y_{O_1} + l_1 \sin \theta_{11} + x \sin(\theta_{11} + \theta_{12}) + \mathbf{S}(x) \mathbf{e} \cos(\theta_{11} + \theta_{12}). \end{aligned}$$

The Jacobian of the point P and velocity of P are calculated as

$$\begin{aligned} \mathbf{r}_P^{(0)} &= \mathbf{r}_P^{(0)}(\mathbf{q}_1) \Rightarrow \mathbf{v}_P^{(0)} = \dot{\mathbf{r}}_P^{(0)}(\mathbf{q}_1) = \mathbf{J}_P(\mathbf{q}_1) \dot{\mathbf{q}}_1 \\ \mathbf{J}_P(\mathbf{q}_1) &= \frac{\partial \mathbf{r}_P^{(0)}(\mathbf{q}_1)}{\partial \mathbf{q}_1}. \end{aligned} \quad (7)$$

The kinetic energy of the elastic link is then determined

$$T_{AE} = \frac{1}{2} \int \mathbf{v}_P^{(0)T} \mathbf{v}_P^{(0)} dm = \frac{1}{2} \frac{m_2}{l_2} \dot{\mathbf{q}}_1^T \left(\int_0^{l_2} \mathbf{J}_P^T(\mathbf{q}_1) \mathbf{J}_P(\mathbf{q}_1) d\zeta \right) \dot{\mathbf{q}}_1 = \frac{1}{2} \dot{\mathbf{q}}_1^T \mathbf{M}_e(\mathbf{q}) \dot{\mathbf{q}}_1.$$

The kinetic energy of the mass at the end point E is determined

$$T_{tip} = \frac{1}{2} m_3 \mathbf{v}_E^{(0)T} \mathbf{v}_E^{(0)} = \frac{1}{2} m_3 \dot{\mathbf{q}}_1^T \mathbf{J}_E^T(\mathbf{q}_1) \mathbf{J}_E(\mathbf{q}_1) \dot{\mathbf{q}}_1 = \frac{1}{2} \dot{\mathbf{q}}_1^T \mathbf{M}_3(\mathbf{q}) \dot{\mathbf{q}}_1.$$

Thus, the kinetic energy of the right part is given by

$$T = \frac{1}{2} I_m \dot{\phi}_1^2 + \frac{1}{2} I_{10} \dot{\theta}_{11}^2 + T_{AE} + T_{tip} = \frac{1}{2} \dot{\mathbf{q}}_1^T [\mathbf{M}_r + \mathbf{M}_e(\mathbf{q}) + \mathbf{M}_3(\mathbf{q})] \dot{\mathbf{q}}_1 = \frac{1}{2} \dot{\mathbf{q}}_1^T \mathbf{M}_1(\mathbf{q}_1) \dot{\mathbf{q}}_1. \quad (8)$$

3.2. Potential energy – generalized forces

Potential energy includes gravity and elastic one. Elastic potential energy of joints and elastic link are given

$$P_e = \frac{1}{2} k (\psi_1 - \theta_{11})^2 + P_{2e} = \frac{1}{2} k (r^{-1} \phi_1 - \theta_{11})^2 + P_{2e}, \quad (9)$$

where $\psi_1 = \phi_1 / r$ is the angular position of the output shaft of the gear box, r is reduction ratio.

To give the element stiffness matrix, the expression of strain potential energy due to transverse bending of the beam needs to be calculated. According to the theory in the strength of materials [28, 29], the bending strain potential energy of a beam is calculated by the formula

$$P_{2e} = \frac{1}{2} \int_0^{l_2} [EI(w'')^2] d\zeta. \quad (10)$$

From (1), we can determine bending strain as

$$d_y = \mathbf{S}(\xi) \mathbf{q}_e \Rightarrow d_y'' = \mathbf{S}''(\xi) \mathbf{q}_e. \quad (11)$$

Substituting (11) into (10) gives

$$P_{2e} = \frac{1}{2} \mathbf{q}_e^T \left(\int_0^{l_2} [EIS''^T(\xi) \mathbf{S}''(\xi)] d\xi \right) \mathbf{q}_e = \frac{1}{2} \mathbf{q}_e^T \mathbf{K}_e \mathbf{q}_e. \quad (12)$$

So, stiffness matrix of the element is obtained

$$\mathbf{K}_e = \int_0^{l_2} [EIS''^T(\xi) \mathbf{S}''(\xi)] d\xi. \quad (13)$$

In combination with the potential energy of torsional spring of the driven shaft:

$$P_e = \frac{1}{2} k (r^{-1} \varphi_1 - \theta_{11})^2 + \frac{1}{2} \mathbf{q}_e^T \mathbf{K}_e \mathbf{q}_e = \frac{1}{2} \mathbf{q}_1^T \mathbf{K}_1 \mathbf{q}_1, \quad (\psi_1 = r^{-1} \varphi_1).$$

And the generalized force of the elastic force is calculated by

$$\left(\frac{\partial P_e}{\partial \mathbf{q}_1} \right)^T = \mathbf{K}_1 \mathbf{q}_1.$$

Potential energy due to gravity

When the manipulator moves in the vertical plane, the potential energy of the weight needs to be added. Let $\mathbf{g}^{(0)} = [g_x, g_y]^T = [0, -g]^T$ be the vector of gravity in a fixed system. If the manipulator moves in a horizontal plane, value of g is set to zero. The gravity potential is calculated as follows

$$P_g = -m_1 \mathbf{g}^{(0)T} \mathbf{r}_{C1}^{(0)}(\mathbf{q}_1) - \frac{m_2}{l_2} \int_0^{l_2} \mathbf{g}^{(0)T} \mathbf{r}_P^{(0)}(\mathbf{q}_1) d\xi - m_3 \mathbf{g}^{(0)T} \mathbf{r}_E^{(0)}(\mathbf{q}_1). \quad (14)$$

The generalized force of gravity is calculated by

$$\begin{aligned} \frac{\partial P_g}{\partial \mathbf{q}} &= -m_1 \mathbf{g}^{(0)T} \frac{\partial}{\partial \mathbf{q}_1} \mathbf{r}_{C1}^{(0)}(\mathbf{q}_1) - m_2 l_2^{-1} \mathbf{g}^{(0)T} \int_0^{l_2} \frac{\partial}{\partial \mathbf{q}_1} \mathbf{r}_P^{(0)} d\xi - m_3 \mathbf{g}^{(0)T} \frac{\partial}{\partial \mathbf{q}_1} \mathbf{r}_E^{(0)}(\mathbf{q}_1) \\ &= -m_1 \mathbf{g}^{(0)T} \mathbf{J}_{T1}(\mathbf{q}_1) - m_2 l_2^{-1} \mathbf{g}^{(0)T} \int_0^{l_2} \mathbf{J}(\mathbf{q}_1) d\xi - m_3 \mathbf{g}^{(0)T} \mathbf{J}_E(\mathbf{q}_1). \end{aligned}$$

Or

$$\left(\frac{\partial P_g}{\partial \mathbf{q}} \right)^T = -m_1 \mathbf{J}_{T1}^T(\mathbf{q}_1) \mathbf{g}^{(0)} - m_2 l_2^{-1} \left(\int_0^{l_2} \mathbf{J}^T(\mathbf{q}) d\xi \right) \mathbf{g}^{(0)} - m_3 \mathbf{J}_E^T(\mathbf{q}_1) \mathbf{g}^{(0)}. \quad (15)$$

Thus, the generalized force due to potential energy can be calculated by the formula

$$\mathbf{g}(\mathbf{q}_1) = \mathbf{K}_1 \mathbf{q}_1 - m_1 \mathbf{J}_{T1}^T(\mathbf{q}_1) \mathbf{g}^{(0)} - m_2 l_2^{-1} \left(\int_0^{l_2} \mathbf{J}^T(\mathbf{q}) d\xi \right) \mathbf{g}^{(0)} - m_3 \mathbf{J}_E^T(\mathbf{q}_1) \mathbf{g}^{(0)}. \quad (16)$$

3.3. Dissipative energy

$$\Phi = \frac{1}{2} c (\psi_1 - \dot{\theta}_{11})^2 + \frac{1}{2} d \dot{\theta}_{11}^2 = \frac{1}{2} c (r^{-1} \dot{\varphi}_1 - \dot{\theta}_{11})^2 + \frac{1}{2} d \dot{\theta}_{11}^2, \quad (17)$$

where d is the viscous coefficient at the bearing O_1 .

3.4. Driving force and constraint forces at the cutting joint

The generalized force of the motor torque acting on the rotor and the force acting at the end point E is calculated based on the calculation of the virtual work as follows:

$$\delta A = \tau_0 \delta \varphi + X \delta x_E + Y \delta y_E = \tau_0 \delta \varphi + [\mathbf{J}_E^T(\mathbf{q}_1) \lambda]^T \delta \mathbf{q}_1,$$

with $\lambda = [X, Y]^T$ and $\mathbf{J}_E(\mathbf{q}_1) = \partial \mathbf{r}_E^{(0)} / \partial \mathbf{q}_1$ is Jacobian of the end point E.

The motor torque acting on the rotor is calculated according to the input current and voltage as follows (here we use the approximate $L_a di/dt \approx 0$)

$$\tau_0 = K_m i = K_m \frac{U - K_e \dot{\varphi}}{R_a} = \frac{K_m}{R_a} U - \frac{K_m K_e}{R_a} \dot{\varphi}. \quad (18)$$

3.5. Equations of motion of the right part

Applying Lagrange's equation of the 2nd kind [30], the differential equation of motion for the right arm would take the form

$$\mathbf{M}_1(\mathbf{q}_1) \ddot{\mathbf{q}}_1 + \mathbf{C}_1(\mathbf{q}_1, \dot{\mathbf{q}}_1) \dot{\mathbf{q}}_1 + \mathbf{D}_1 \dot{\mathbf{q}}_1 + \mathbf{K}_1 \mathbf{q}_1 + \mathbf{g}_1(\mathbf{q}_1) = \mathbf{B}_1 \mathbf{u}_1 + \mathbf{J}_{E1}^T \lambda, \quad (19)$$

where $\mathbf{M}_1(\mathbf{q}_1)$ is the mass matrix of size 5×5 that is the Hessian matrix of kinetic energy with respect to $\dot{\mathbf{q}}$; \mathbf{D}_1 is the damping matrix; Lagrange multipliers $\lambda = [X, Y]^T$ are the reaction forces at cutting joint E; the Coriolis and centrifugal matrix $\mathbf{C}_1(\mathbf{q}_1, \dot{\mathbf{q}}_1)$ are determined from the mass matrix $\mathbf{M}_1(\mathbf{q}_1)$ based on Kronecker product [31] or by the Christoffel formula

$$\mathbf{C}_1(\mathbf{q}_1, \dot{\mathbf{q}}_1) = \{c_{ij}(\mathbf{q}_1, \dot{\mathbf{q}}_1)\}, \quad c_{ij}(\mathbf{q}_1, \dot{\mathbf{q}}_1) = \frac{1}{2} \sum_{k=1}^m \left(\frac{\partial m_{ij}}{\partial q_k} + \frac{\partial m_{ik}}{\partial q_j} - \frac{\partial m_{jk}}{\partial q_i} \right) \dot{q}_k. \quad (20)$$

Normally, the differential equation of motion for a serial flexible manipulator is written in the following form

$$\begin{aligned} & \begin{bmatrix} \mathbf{M}_{rr}(\mathbf{q}) & \mathbf{M}_{rf}(\mathbf{q}) \\ \mathbf{M}_{fr}(\mathbf{q}) & \mathbf{M}_{ff}(\mathbf{q}) \end{bmatrix} \begin{bmatrix} \ddot{\mathbf{q}}_r \\ \ddot{\mathbf{q}}_f \end{bmatrix} + \begin{bmatrix} \mathbf{C}_{rr}(\mathbf{q}, \dot{\mathbf{q}}) & \mathbf{C}_{rf}(\mathbf{q}, \dot{\mathbf{q}}) \\ \mathbf{C}_{fr}(\mathbf{q}, \dot{\mathbf{q}}) & \mathbf{C}_{ff}(\mathbf{q}, \dot{\mathbf{q}}) \end{bmatrix} \begin{bmatrix} \dot{\mathbf{q}}_r \\ \dot{\mathbf{q}}_f \end{bmatrix} \\ & + \begin{bmatrix} \mathbf{D}_{rr} & \mathbf{0} \\ \mathbf{0} & \mathbf{0} \end{bmatrix} \begin{bmatrix} \dot{\mathbf{q}}_r \\ \dot{\mathbf{q}}_f \end{bmatrix} + \begin{bmatrix} \mathbf{K}_{rr} & \mathbf{0} \\ \mathbf{0} & \mathbf{K}_{ff} \end{bmatrix} \begin{bmatrix} \mathbf{q}_r \\ \mathbf{q}_f \end{bmatrix} + \begin{bmatrix} \mathbf{g}_r(\mathbf{q}) \\ \mathbf{g}_f(\mathbf{q}) \end{bmatrix} = \begin{bmatrix} \mathbf{B}_r U \\ \mathbf{0} \end{bmatrix} + \begin{bmatrix} \Phi_r^T \\ \Phi_f^T \end{bmatrix} \lambda. \end{aligned} \quad (21)$$

For the given manipulator, these matrices and vectors are written in detail as follows

$$\mathbf{M}_{rr}(\mathbf{q}) = \begin{bmatrix} I_m & 0 & 0 \\ 0 & m_{22} & m_{23} \\ 0 & m_{32} & m_{33} \end{bmatrix}, \quad \mathbf{M}_{fr} = \mathbf{M}_{rf}^T,$$

$$m_{22} = I_1 + \frac{13}{35}m_2e_3^2 - \frac{11}{105}m_2e_3e_4l_2 + \frac{1}{105}m_2e_4^2l_2^2 - m_2l_1e_3 \sin q_2 + \frac{1}{6}m_2l_1l_2e_4 \sin q_2 \\ + \frac{1}{3}m_2l_2^2 + m_2l_1 \cos q_2l_2 + m_2l_1^2 + m_3(l_1^2 + l_2^2 + 2l_1l_2 \cos q_2 - 2l_1e_3 \sin q_2 + e_3^2),$$

$$m_{32} = m_{23} = \frac{13}{35}m_2e_3^2 - \frac{11}{105}m_2e_3e_4l_2 + \frac{1}{105}m_2e_4^2l_2^2 - \frac{1}{2}m_2l_1 \sin q_2e_3 + \frac{1}{12}m_2l_1l_2e_4 \sin q_2 \\ + \frac{1}{3}m_2l_2^2 + \frac{1}{2}m_2l_1l_2 \cos q_2 + m_3(l_1l_2 \cos q_2 - l_1e_3 \sin q_2 + l_2^2 + e_3^2),$$

$$m_{33} = \frac{13}{35}m_2e_3^2 - \frac{11}{105}m_2e_3e_4l_2 + \frac{1}{105}m_2e_4^2l_2^2 + \frac{1}{3}m_2l_2^2 + m_3(l_2^2 + e_3^2),$$

$$\mathbf{M}_{fr} = \begin{bmatrix} 0 & \frac{7}{20}m_2l_2 + \frac{1}{2}m_2l_1 \cos q_2 + m_3(l_1 \cos q_2 + l_2) & \frac{7}{20}m_2l_2 + m_3l_2 \\ 0 & -\frac{1}{20}m_2l_2^2 - \frac{1}{12}m_2l_1l_2 \cos q_2 & -\frac{1}{20}m_2l_2^2 \end{bmatrix},$$

$$\mathbf{M}_{ff} = \begin{bmatrix} \frac{13}{35}m_2 + m_3 & -\frac{11}{210}m_2l_2 \\ -\frac{11}{210}m_2l_2 & \frac{1}{105}m_2l_2^2 \end{bmatrix}$$

$$\mathbf{D}_{rr} = \begin{bmatrix} c/r^2 + K_m K_e / R_a & -c/r & 0 \\ -c/r & c & 0 \\ 0 & 0 & 0 \end{bmatrix}, \quad \mathbf{D}_{fr} = \mathbf{0}_{2 \times 3}, \quad \mathbf{D}_{ff} = \mathbf{0}_{3 \times 3},$$

$$\mathbf{K}_{rr} = \begin{bmatrix} k/r^2 & -k/r & 0 \\ -k/r & k & 0 \\ 0 & 0 & 0 \end{bmatrix}, \quad \mathbf{K}_{fr} = \mathbf{0}_{2 \times 3}, \quad \mathbf{K}_{ff} = \begin{bmatrix} 12EI/l_2^3 & -6EI/l_2^2 \\ -6EI/l_2^2 & 4EI/l_2 \end{bmatrix},$$

$$g_1(\mathbf{q}) = 0,$$

$$g_2(\mathbf{q}) = m_1s_1g \cos q_1 + \frac{1}{12}m_2[-6e_3 \sin(q_1 + q_2) + e_4l_2 \sin(q_1 + q_2) + 6l_2 \cos(q_1 + q_2) \\ + 12l_1 \cos q_1]g + m_3[l_1 \cos q_1 + l_2 \cos(q_1 + q_2) - e_3 \sin(q_1 + q_2)]g,$$

$$g_3(\mathbf{q}) = \frac{1}{12}m_2[-6e_3 \sin(q_1 + q_2) + e_4l_2 \sin(q_1 + q_2) + 6l_2 \cos(q_1 + q_2)]g \\ + m_3[l_2 \cos(q_1 + q_2) - e_3 \sin(q_1 + q_2)]g,$$

$$g_4(\mathbf{q}) = (\frac{1}{2}m_2 + m_3) \cos(q_1 + q_2)g, \quad g_5(\mathbf{q}) = -\frac{1}{12}m_2l_2 \cos(q_1 + q_2)g,$$

$$\mathbf{B}_{rr} = [K_m/R_a \quad 0 \quad 0]^T.$$

The equation of motion for the rotor is obtained after neglecting the current changing, it means $L_a di/dt \approx 0$:

$$I_m \ddot{\varphi} + \left(\frac{c}{r^2} + \frac{K_m K_e}{R_a} \right) \dot{\varphi} - \frac{c}{r} \dot{\theta} + \left(\frac{k}{r^2} \right) \varphi - \frac{k}{r} \theta = \frac{K_m}{R_a} U.$$

3.6. Constraint equations

With the given generalized coordinates, the constraint equations are obtained by comparison between the position of the endpoints E of the right and left parts

$$\boldsymbol{\phi}(\mathbf{q}_1, \mathbf{q}_2) = \mathbf{r}_{E1}^{(0)}(\mathbf{q}_1) - \mathbf{r}_{E2}^{(0)}(\mathbf{q}_2) = \mathbf{0}, \quad (22)$$

in which for the right part

$$\begin{aligned} x_{E1}^{(0)} &= x_{O1} + l_1 \cos \theta_{11} + l_2 \cos(\theta_{11} + \theta_{12}) - e_{13} \sin(\theta_{11} + \theta_{12}), \\ y_{E1}^{(0)} &= y_{O1} + l_1 \sin \theta_{11} + l_2 \sin(\theta_{11} + \theta_{12}) + e_{13} \cos(\theta_{11} + \theta_{12}), \end{aligned}$$

and for the left part

$$\begin{aligned} x_{E2}^{(0)} &= x_{O2} + l_1 \cos \theta_{21} + l_2 \cos(\theta_{21} + \theta_{22}) - e_{23} \sin(\theta_{21} + \theta_{22}), \\ y_{E2}^{(0)} &= y_{O2} + l_1 \sin \theta_{21} + l_2 \sin(\theta_{21} + \theta_{22}) + e_{23} \cos(\theta_{21} + \theta_{22}). \end{aligned}$$

3.7. Dynamic equations of the whole system

Combining the equations of two parts together gives the dynamic equations of the whole system in the form of differential algebraic equations (DAEs) as following

$$\begin{aligned} \mathbf{M}(\mathbf{q})\ddot{\mathbf{q}} + \mathbf{C}(\mathbf{q}, \dot{\mathbf{q}})\dot{\mathbf{q}} + \mathbf{D}\dot{\mathbf{q}} + \mathbf{K}\mathbf{q} + \mathbf{g}(\mathbf{q}) &= \mathbf{B}\mathbf{u} + \Phi_q^T \boldsymbol{\lambda}, \\ \boldsymbol{\phi}(\mathbf{q}) = \mathbf{r}_{Er}(\mathbf{q}) - \mathbf{r}_{El}(\mathbf{q}) &= \mathbf{0}, \quad \Phi_q = \partial \boldsymbol{\phi}(\mathbf{q}) / \partial \mathbf{q}. \end{aligned} \quad (23)$$

The matrices and vectors in (23) are given as

$$\begin{aligned} \mathbf{M}(\mathbf{q}) &= \text{diag}([\mathbf{M}_1(\mathbf{q}), \mathbf{M}_2(\mathbf{q})]), & \mathbf{C}(\mathbf{q}, \dot{\mathbf{q}}) &= \text{diag}([\mathbf{C}_1(\mathbf{q}, \dot{\mathbf{q}}), \mathbf{C}_2(\mathbf{q}, \dot{\mathbf{q}})]), \\ \mathbf{D} &= \text{diag}([\mathbf{D}_1, \mathbf{D}_2]), & \mathbf{K} &= \text{diag}([\mathbf{K}_1, \mathbf{K}_2]), \\ \mathbf{g}(\mathbf{q}) &= [\mathbf{g}_1^T(\mathbf{q}), \mathbf{g}_2^T(\mathbf{q})]^T, & \mathbf{B} &= [\mathbf{B}_1, 0; 0, \mathbf{B}_2], \\ \mathbf{u} &= [U_1, U_2]^T, & \boldsymbol{\lambda} &= [X, Y]^T, \quad \Phi_q^T = [\mathbf{J}_{E1}^T; \mathbf{J}_{E2}^T]. \end{aligned}$$

4. NUMERICAL SIMULATION OF FORWARD DYNAMICS

4.1. Forward dynamics

Forward dynamics of flexible parallel manipulators are solved in the same way as of rigid parallel manipulators. There are some methods to determine generalized acceleration $\ddot{\mathbf{q}}$ from equations of motion (23). In this study, the second derivatives of the constraint equations is used and the matrix \mathbf{R} satisfying $\mathbf{R}^T \Phi^T = \mathbf{0}$ is exploited to eliminate the Lagrangian multipliers. Additionally, to restrict the drift of constraint equations during integration, the Baumgarte's stabilization technique is applied [32]. So, the dynamic equations for forward dynamics will be as following

$$\begin{aligned} \mathbf{R}^T \mathbf{M}(\mathbf{q})\ddot{\mathbf{q}} &= \mathbf{R}^T (\mathbf{B}\mathbf{u} - \mathbf{C}(\mathbf{q}, \dot{\mathbf{q}})\dot{\mathbf{q}} - \mathbf{D}\dot{\mathbf{q}} - \mathbf{K}\mathbf{q} - \mathbf{g}(\mathbf{q})), \\ \boldsymbol{\Phi}(\mathbf{q})\ddot{\mathbf{q}} &= -\dot{\boldsymbol{\Phi}}(\mathbf{q})\dot{\mathbf{q}} - 2\delta\omega\boldsymbol{\Phi}(\mathbf{q})\dot{\mathbf{q}} - \omega^2\boldsymbol{\phi}(\mathbf{q}), \quad \delta, \omega > 0. \end{aligned}$$

Solving the above equations for $\ddot{\mathbf{q}}$ gives

$$\ddot{\mathbf{q}} = \begin{bmatrix} \mathbf{R}^T \mathbf{M}(\mathbf{q}) \\ \boldsymbol{\Phi}(\mathbf{q}) \end{bmatrix}^{-1} \begin{bmatrix} \mathbf{R}^T (\mathbf{B}\mathbf{u} - \mathbf{C}(\mathbf{q}, \dot{\mathbf{q}})\dot{\mathbf{q}} - \mathbf{D}\dot{\mathbf{q}} - \mathbf{K}\mathbf{q} - \mathbf{g}(\mathbf{q})) \\ -\dot{\boldsymbol{\Phi}}(\mathbf{q})\dot{\mathbf{q}} - 2\delta\omega\boldsymbol{\Phi}(\mathbf{q})\dot{\mathbf{q}} - \omega^2\boldsymbol{\phi}(\mathbf{q}) \end{bmatrix}. \quad (24)$$

The motion of the system is obtained by integration (24) with the consistent initial conditions, that satisfy the constraint equations at the position and velocity level.

4.2. Simulation results

In this subsection, the simulation results on five-bar parallel manipulator with flexible link and joints are presented. The kinematic and dynamic parameters of the system shown in Fig. 1 are chosen as in Table 1.

Table 1. System parameters

Actuator and gear transmission	
$K_m = 1;$	Nm/A, torque constant
$K_e = 1;$	Volt.s/rad, BACK-EMF constant
$R_a = 3;$	Ohm, armature resistance of the motor
$I_m = 0.1;$	kgm ² , moment of inertia of the rotor
$r = -10;$	-, gearbox ratio
$k = 5000;$	Nm/rad, torsional stiffness of the spring
$c = k/100;$	Nms/rad, viscous coefficient
Rigid link 1	
$m_1 = 3;$	kg, mass
$l_1 = 0.4;$	m, length
$s_1 = 0.2;$	m, center of mass, OC1
$I_1 = 0.2;$	kgm ² , moment of inertia about axis 0
Flexible link 2	
$\rho = 2712;$	kg/m ³ , mass density
$E = 7.102 * 10^{10};$	N/m ² , elastic module
$l_2 = 0.5;$	m, length
$h = 0.003;$	m, thickness
$b = 0.030;$	m, width
$A = b * h;$	m ² cross-sectional area
$I = b * h^3 / 12;$	m ⁴ , area moment of inertia
$m_2 = \rho * l_2 * b * h;$	kg, mass
$L_0 = 0.6;$	m, distance O_1O_2
$m_3 = 0.25;$	kg, 1/2 mass at the end-effector
$g = 9.81;$	m/s ² , gravity acceleration
Baumgarte parameters: $\delta = 1, \omega = 700$	

In the simulation, the voltage applied to the motor is chosen as PD controller plus gravity

$$\begin{aligned} \text{upd} &= [72 * (2 * r - q(1)) - 30 * \text{qdot}(1); 72 * (2 * r - q(6)) - 30 * \\ &\quad \text{qdot}(6)]; \\ \text{ug} &= \text{pinv}(R' * B) * R' * (G); \\ \text{u} &= \text{upd} + \text{ug}; \end{aligned}$$

The consistent initial conditions are calculated based on the rigid model of the manipulator, deformation of the flexible links are disregarded

```

q0 = [* 0.9812 1.5958, 0 0, * 1.7125 -1.2922, 0 0]';
q0(1) = q0(2)*r; % torsional spring 1 is relax;
q0(6) = q0(7)*r; % torsional spring 2 is relax;
dq0 = [0 0 0, 0 0, 0 0 0, 0 0]';
    
```

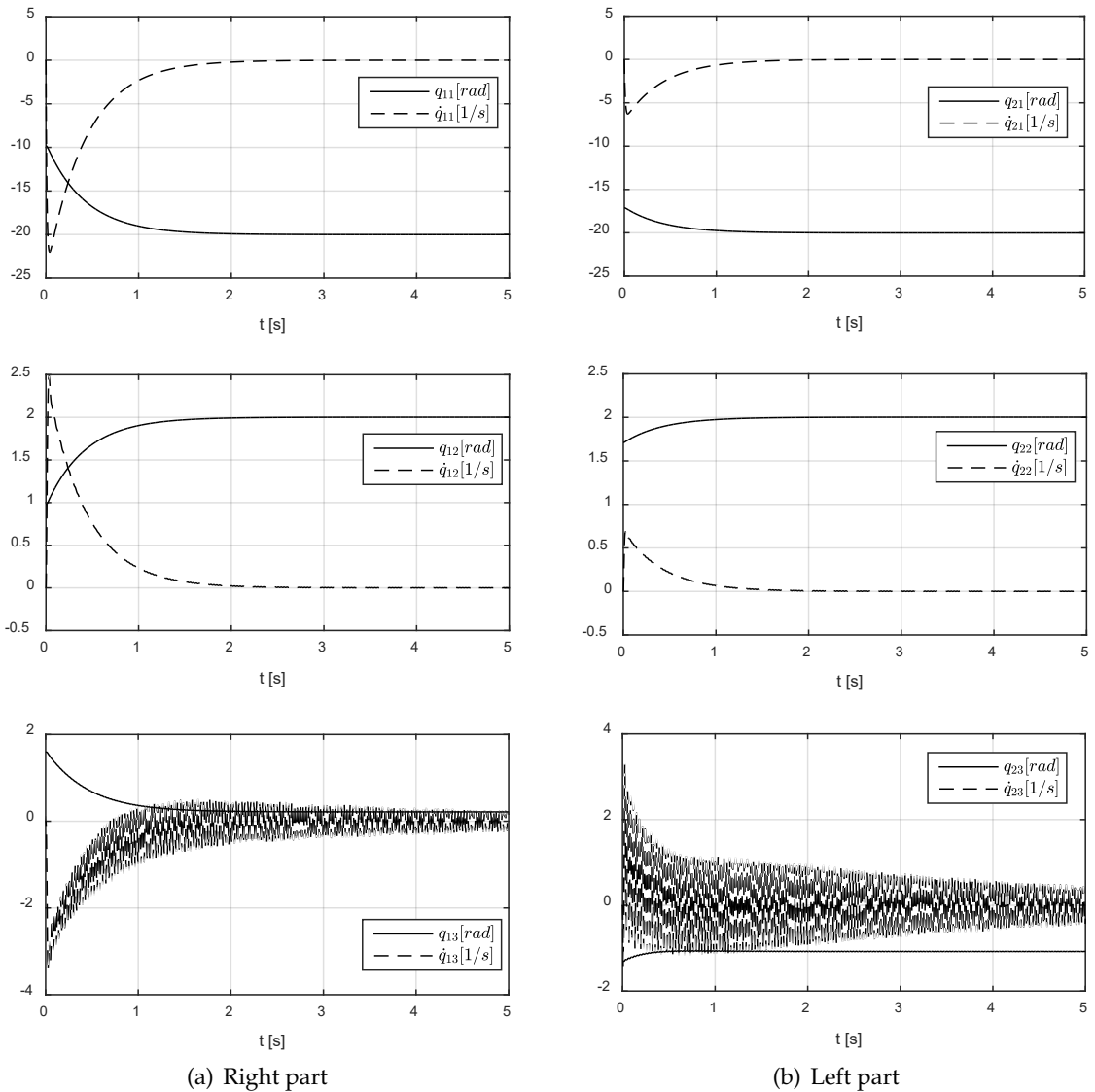


Fig. 4. Time history of joint variables (solid line: position; dashed line: velocity)

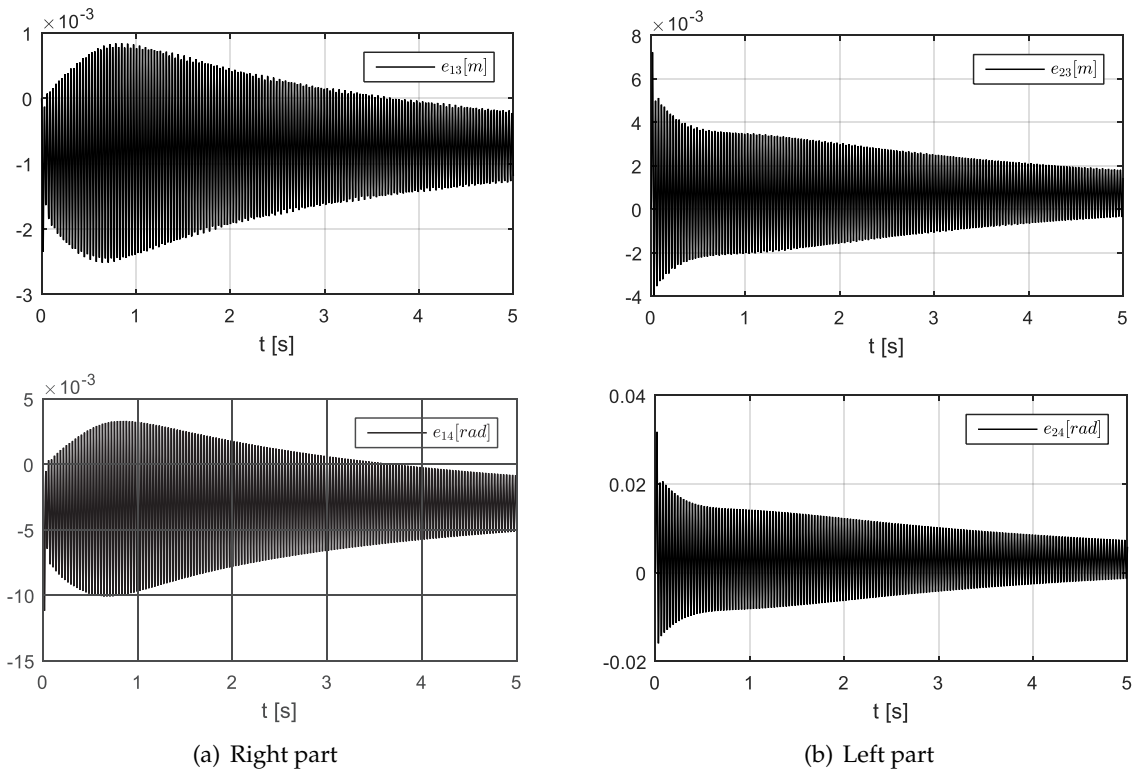


Fig. 5. Time history of transverse and angular deflection of flexible links

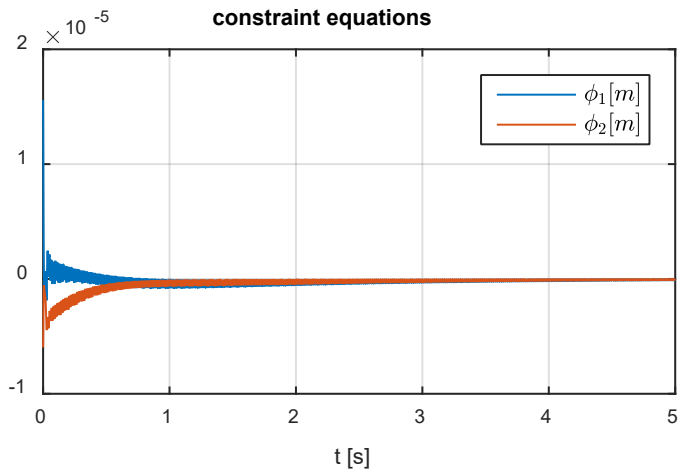


Fig. 6. Time history of error of constraint equations

The simulation results are shown in Fig. 4 and Fig. 5 include time plots of the joint variables of the rigid link and the deflection of the flexible link. The graph of the joint variables q_{11}, q_{12}, q_{13} and q_{21}, q_{22}, q_{23} reaches the stationary position after about 2.5 s (Fig. 4). The deformation motion graph $e_{13}, e_{14}, e_{23}, e_{24}$ shows high frequency oscillation even when the manipulator has reached the target position (Fig. 5). The oscillation of the flexible link has a clear effect on the joint variables q_{13} and q_{23} . The graph in Fig. 6 shows that with Baumgarte stabilization, the errors of the constraint equations are kept small and approaches zero as the manipulator comes to rest.

5. CONCLUSIONS

An approach to establish dynamic models of parallel robotic manipulators with rigid and flexible links and elastic joints is presented. According to the symmetric structure of the parallel robot, the system is divided into some similar substructures consisting of components with lumped parameters (rigid bodies and springs) and distributed parameters (flexible links). The flexible links are modeled by beams subjected to flexural deflection and using a method of floating reference frames. Based on kinetic energy, potential energy and dissipative energy, dynamic equations are established for each substructure using Lagrange's equation of 2nd kind. The overall equations obtained form a system of algebraic differential equations. These equations are solved by Lagrange multiplier elimination and combined with Baumgarte stabilization technique to ensure that the constraint is not broken in numerical simulation. The approach in this paper can be applied to modeling parallel planar and spatial robots with flexible links and elastic joints.

DECLARATION OF COMPETING INTEREST

The authors declare that they have no known competing financial interests or personal relationships that could have appeared to influence the work reported in this paper.

FUNDING

This research received no specific grant from any funding agency in the public, commercial, or not-for-profit sectors.

REFERENCES

- [1] A. A. Shabana. *Multibody System Dynamics*, **1**, (2), (1997), pp. 189–222. <https://doi.org/10.1023/a:1009773505418>.
- [2] S. K. Dwivedy and P. Eberhard. Dynamic analysis of flexible manipulators, a literature review. *Mechanism and Machine Theory*, **41**, (2006), pp. 749–777. <https://doi.org/10.1016/j.mechmachtheory.2006.01.014>.
- [3] K. Lochan, B. K. Roy, and B. Subudhi. A review on two-link flexible manipulators. *Annual Reviews in Control*, **42**, (2016), pp. 346–367. <https://doi.org/10.1016/j.arcontrol.2016.09.019>.
- [4] Y. Gao, F.-Y. Wang, and Z.-Q. Zhao. *Flexible manipulators: Modeling, analysis and optimum design*. Academic Press, (2012).

- [5] R. E. Valembois, P. Fisette, and J. C. Samin. Comparison of various techniques for modelling flexible beams in multibody dynamics. *Nonlinear Dynamics*, **12**, (4), (1997), pp. 367–397. <https://doi.org/10.1023/a:1008204330035>.
- [6] T. M. Wasfy and A. K. Noor. Computational strategies for flexible multibody systems. *Applied Mechanics Reviews*, **56**, (2003), pp. 553–613. <https://doi.org/10.1115/1.1590354>.
- [7] M. Benosman and G. Le Vey. Joint trajectory tracking for planar multi-link flexible manipulator: Simulation and experiment for a two-link flexible manipulator. In *Proceedings 2002 IEEE International Conference on Robotics and Automation (Cat. No. 02CH37292)*, IEEE, Vol. 3, (2002), pp. 2461–2466.
- [8] R. Seifried. *Dynamics of underactuated multibody systems*. Springer International Publishing, (2014). <https://doi.org/10.1007/978-3-319-01228-5>.
- [9] N. Q. Hoang. Effect of motion law on driving torque and oscillation of manipulators with flexible links. In *the proceedings of 10th National Conference of Mechanics, Volume 2, Dynamics and Controls*, (2017). (in Vietnamese).
- [10] D. C. Dat, N. V. Khang, N. Q. Hoang, and N. V. Quyen. Stability control of dynamical systems described by linear differential equations with time-periodic coefficients. In *Advances in Asian Mechanism and Machine Science*. Springer International Publishing, (2021), pp. 489–500. https://doi.org/10.1007/978-3-030-91892-7_46.
- [11] C. A. My and D. X. Bien. New development of the dynamic modeling and the inverse dynamic analysis for flexible robot. *International Journal of Advanced Robotic Systems*, **17**, (4), (2020).
- [12] S. Briot and W. Khalil. *Dynamics of parallel robots: from rigid bodies to flexible elements. Mechanisms and machine science*. Springer, Berlin, (2015).
- [13] N. V. Khang, N. S. Nam, and N. P. Dien. Modelling and model-based control of a four-bar mechanism with a flexible coupler link. In *Robotics and Mechatronics*. Springer International Publishing, (2019), pp. 67–81. https://doi.org/10.1007/978-3-030-17677-8_6.
- [14] Q. Zhang, X. Fan, and X. Zhang. Dynamic analysis of planar 3-RRR flexible parallel robots with dynamic stiffening. *Shock and Vibration*, **2014**, (2014), pp. 1–13. <https://doi.org/10.1155/2014/370145>.
- [15] D. Zhaocai and Y. Yueqing. Dynamic modeling and inverse dynamic analysis of flexible parallel robots. *International Journal of Advanced Robotic Systems*, **5**, (2008). <https://doi.org/10.5772/5654>.
- [16] C. Zhengsheng, K. Minxiu, L. Ming, and Y. Wei. Dynamic modelling and trajectory tracking of parallel manipulator with flexible link. *International Journal of Advanced Robotic Systems*, **10**, (2013). <https://doi.org/10.5772/56765>.
- [17] S.-M. Kim. Lumped element modeling of a flexible manipulator system. *IEEE/ASME Transactions on Mechatronics*, **20**, (2015), pp. 967–974. <https://doi.org/10.1109/tmech.2014.2327070>.
- [18] H. Cervantes-Culebro, J. E. Chong-Quero, E. A. Padilla-Garcia, and C. A. Cruz-Villar. Concurrent design of a 2 DOF five-bar parallel robot a hybrid design of rigid and flexible links. *IEEE Access*, **9**, (2021), pp. 17450–17462. <https://doi.org/10.1109/access.2021.3053250>.
- [19] Z.-C. Qiu. Adaptive nonlinear vibration control of a Cartesian flexible manipulator driven by a ballscrew mechanism. *Mechanical Systems and Signal Processing*, **30**, (2012), pp. 248–266. <https://doi.org/10.1016/j.ymssp.2012.01.002>.
- [20] M. Dadfarnia, N. Jalili, B. Xian, and D. M. Dawson. Lyapunov-based vibration control of translational Euler-Bernoulli beams using the stabilizing effect of beam damping mechanisms. *Journal of Vibration and Control*, **10**, (2004), pp. 933–961. <https://doi.org/10.1177/1077546304042070>.

- [21] H. Yang, H. Krishnan, and M. H. Ang. A simple rest-to-rest control command for a flexible link robot. In *Proceedings of International Conference on Robotics and Automation*, IEEE, Vol. 4, (1997), pp. 3312–3317. <https://doi.org/10.1109/ROBOT.1997.606794>.
- [22] M. Benosman, G. L. Vey, L. Lanari, and A. D. Luca. Rest-to-rest motion for planar multi-link flexible manipulator through backward recursion. *Journal of Dynamic Systems, Measurement, and Control*, **126**, (2004), pp. 115–123. <https://doi.org/10.1115/1.1649976>.
- [23] I. M. M. Lammerts. *Adaptive computed reference computed torque control of flexible manipulators*. Technische Universiteit Eindhoven, (1993). <https://doi.org/10.6100/IR402510>.
- [24] Y. Tang, F. Sun, and Z. Sun. Neural network control of flexible-link manipulators using sliding mode. *Neurocomputing*, **70**, (2006), pp. 288–295. <https://doi.org/10.1016/j.neucom.2006.01.030>.
- [25] N. V. Khang and D. C. Dat. Vibration control and calculating inverse dynamics of the rigid-flexible two-link manipulator T-R. *Vietnam Journal of Mechanics*, **44**, (2022), pp. 169–189. <https://doi.org/10.15625/0866-7136/16876>.
- [26] J. G. de Jalón and E. Bayo. *Kinematic and dynamic simulation of multibody systems*. Springer New York, (1994). <https://doi.org/10.1007/978-1-4612-2600-0>.
- [27] P. B. Usoro, R. Nadira, and S. S. Mahil. A finite element/lagrange approach to modeling lightweight flexible manipulators. *Journal of Dynamic Systems, Measurement, and Control*, **108**, (1986), pp. 198–205. <https://doi.org/10.1115/1.3143768>.
- [28] C. Q. Thang. *Finite element method*. Science and Technics Publishing House, Hanoi, (1997). (in Vietnamese).
- [29] T. I. Thinh and N. N. Khoa. *Finite element method*. Science and Technics Publishing House, Hanoi, (2007). (in Vietnamese).
- [30] N. V. Khang. *Dynamics of multibody systems*. Science and Technics Publishing House, Hanoi, (2017). (in Vietnamese).
- [31] N. V. Khang. Kronecker product and a new matrix form of Lagrangian equations with multipliers for constrained multibody systems. *Mechanics Research Communications*, **38**, (2011), pp. 294–299. <https://doi.org/10.1016/j.mechrescom.2011.04.004>.
- [32] J. Baumgarte. Stabilization of constraints and integrals of motion in dynamical systems. *Computer Methods in Applied Mechanics and Engineering*, **1**, (1972), pp. 1–16. [https://doi.org/10.1016/0045-7825\(72\)90018-7](https://doi.org/10.1016/0045-7825(72)90018-7).